

# Recent Results from the H1 Collaboration

Stefan Schmitt<sup>1</sup> \*

DESY Hamburg  
Notkestraße 85, 22607 Hamburg - Germany

An overview of recent physics results from the H1 collaboration is given. The covered areas are: rare processes and searches for new physics, structure functions and inclusive measurements, heavy flavour production, QCD and hadronic final states, diffractive scattering.

## 1 Introduction

During the years 1994–2007 the HERA  $ep$  collider in Hamburg collided electrons or positrons with an energy of 27.5 GeV and protons with an energy of 920 GeV, at a centre-of-mass energy of 320 GeV<sup>a</sup>. The last months of data taking were dedicated to special low energy runs, with proton energies of 460 and 575 GeV, corresponding to centre-of-mass energies of 220 and 250 GeV, respectively. During the whole data taking period, the H1 detector recorded almost  $200 \text{ pb}^{-1}$  in  $e^-p$  collisions and almost  $300 \text{ pb}^{-1}$  in  $e^+p$  collisions at high centre-of-mass energy. These data are now fully exploited to achieve milestones of the HERA physics program. A few recent results are presented here [1].

## 2 Rare processes and searches for new physics

At HERA,  $W$  bosons may be singly produced in the reaction  $e^\pm p \rightarrow e^\pm W X$ . Leptonic decays of the  $W$  bosons lead to the spectacular signatures of a high momentum isolated lepton and missing transverse momentum due to the decay neutrino. Such events are measured by H1 [2] as a function of the transverse momentum of the hadronic system  $P_T^X$ . At large  $P_T^X > 25 \text{ GeV}$  an excess of 17 observed over  $8.0 \pm 1.3$  expected events is seen in  $e^+p$  scattering. In  $e^-p$  scattering only 1 event is seen, with  $5.6 \pm 0.9$  expected from the Standard Model (SM). The transverse mass distribution of the isolated lepton and the neutrino exhibits a shape with a falling edge above 80 GeV, as expected from  $W$  decays. The production cross-section of single  $W$  at HERA is measured as a function of  $P_T^X$  and is shown in Figure 1, together with the observed transverse mass distribution. A total cross-section of  $1.14 \pm 0.25 \pm 0.14 \text{ pb}^{-1}$  is found.

Events with several high  $P_T$  leptons ( $e$  or  $\mu$ ) are also investigated. Within the SM such events are predominantly produced from  $\gamma\gamma$  collisions. The H1 and ZEUS collaboration both measure individually these topologies [3, 4]. In order to enhance the sensitivity to new phenomena, a combined H1 and ZEUS analysis is performed [5] in a common phase-space. Multi-lepton events are observed at high scalar sum of transverse momentum  $\sum p_T > 100 \text{ GeV}$ . In  $e^+p$  collisions, 7 events are observed for  $1.94 \pm 0.17$  expected, whereas in  $e^-p$  collisions no event is seen, for  $1.19 \pm 0.12$  expected. The cross-section for multi-lepton production is measured as a function of the scalar sum of the lepton  $P_T$  and as a function of the invariant mass, as depicted in Figure 2.

\*On behalf of the H1 Collaboration

<sup>a</sup>A small fraction of the data was taken with a proton energy of 820 GeV.

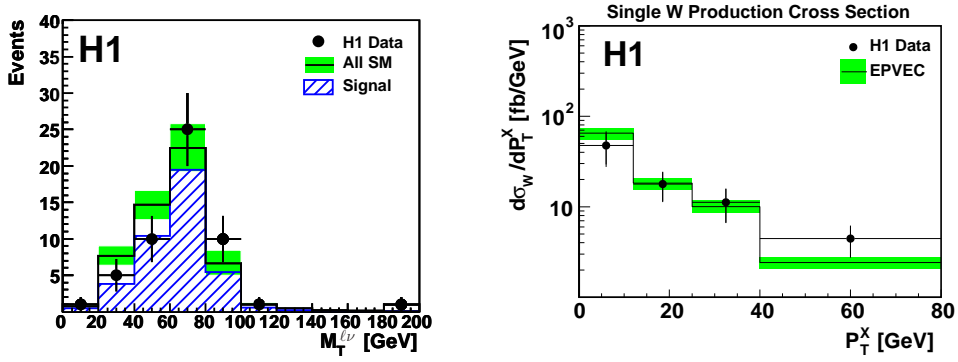


Figure 1: Single W production at HERA

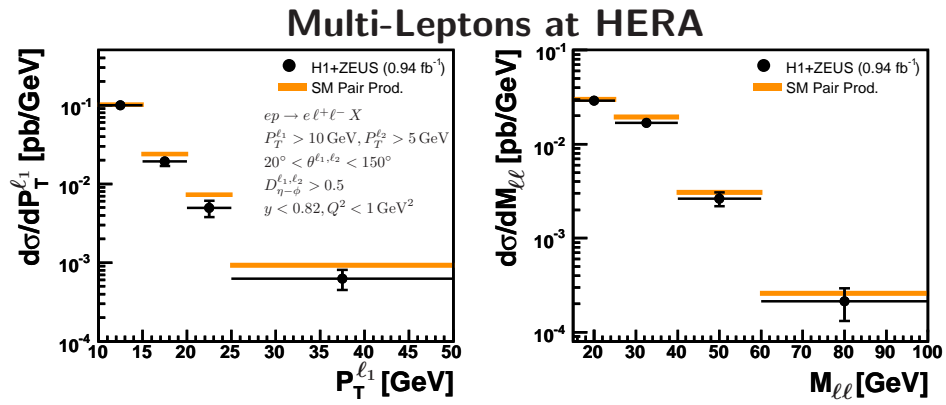


Figure 2: Multi-lepton production at HERA

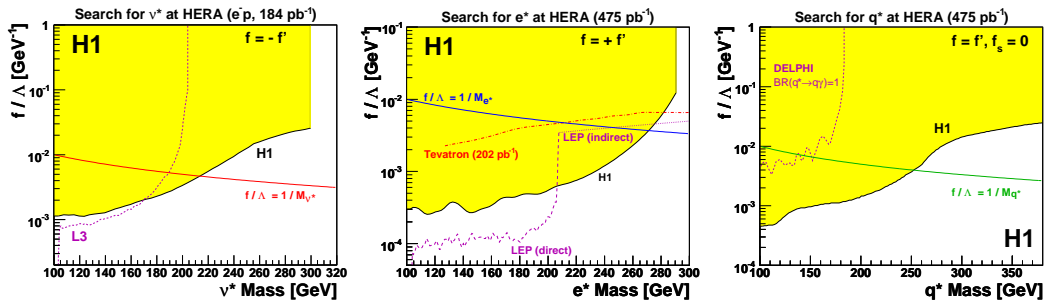


Figure 3: Exclusion limits on excited fermion production at HERA

The H1 data also have been searched for excited fermions. Mass-dependent limits on the coupling  $f/\Lambda$  for the production of excited neutrinos [6], excited electrons [7] and excited quarks [8] are shown in Figure 3. The excited quark limits are derived with the additional assumption  $f_s = 0$ , complementary to TeVatron searches, where  $f_s = f$  is assumed. Using the conventional assumption  $\Lambda/f = m_{f^*}$ , masses  $m_{\nu^*} < 213$  GeV,  $m_{e^*} < 272$  GeV and  $m_{q^*} < 252$  GeV are excluded at 95% CL.

### 3 Structure functions and inclusive measurements

The measurement of structure functions is one of the key elements of HERA physics. Recent analysis from H1 reach unprecedented accuracy in this area. The data at low momentum transfer  $Q^2 \lesssim 12$  GeV, have a precision of 2 – 3 percent [9]. In Figure 4 they are compared to phenomenological models based on the dipole approach and good agreement is found. At

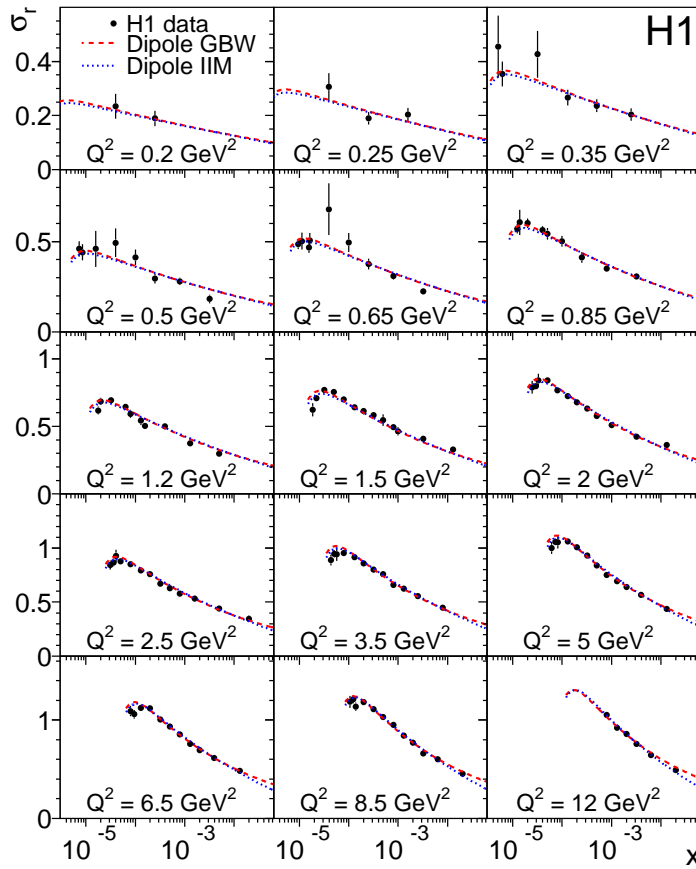


Figure 4: The reduced cross-section  $\sigma_r$  at low  $Q^2$

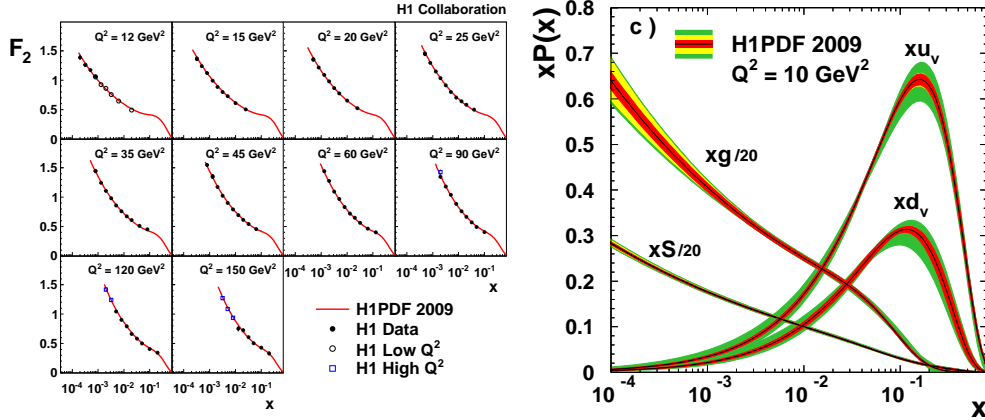


Figure 5: The structure function  $F_2$  (left) and the parton distribution functions obtained from the H1PDF2009 fit (right)

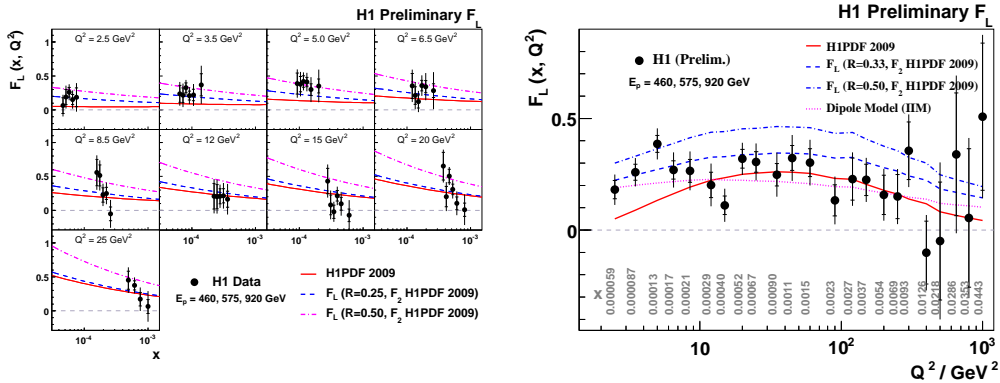


Figure 6: The longitudinal structure function  $F_L$ , as a function of  $x$  and  $Q^2$  (left) and as a function of  $Q^2$ , averaged over the corresponding  $x$  values (right)

medium  $Q^2$  up to 150 GeV the precision reaches 1.3–2% [10]. A NLO QCD fit (H1PDF2009) of the complete H1 data collected up to the year 2000 is performed and parton densities are extracted. The new data are described very well by the QCD fit. The extracted parton densities have much reduced errors, as compared to earlier fits. The new data on the structure function  $F_2$  and the results of the H1PDF2009 fit are shown in Figure 5. Three error sources are indicated on the fit results: the innermost error band are experimental errors, followed by theory uncertainties. The outermost error band includes the uncertainty due the PDF parametrisation, which is defined here for the first time.

Using the data collected in dedicated low energy runs, a direct measurement of the longitudinal structure function  $F_L$  is performed. Data collected at medium  $Q^2$  [11] are

combined with measurements at lower and higher  $Q^2$  and together cover the kinematic range  $2.5 Q^2 < 800 \text{ GeV}^2$ . The results are shown in Figure 6. The new data at low  $Q^2$  are shown as a function of  $x$  and  $Q^2$ . All H1 data for a given  $Q^2$  are then averaged over  $x$  and the result is shown as a function of  $Q^2$ . The data are compared to predictions of the H1PDF2009 QCD fit and to a dipole model. At small  $Q^2$  the  $F_L$  predicted from the QCD fit is lower than observed, whereas the dipole model is found to be in agreement with the data. The data has a good potential to constrain the models of the proton structure at low  $x$ .

## 4 Heavy flavour production

Charm and beauty quarks are produced at HERA predominantly in the boson gluon fusion process, where the virtual photon and a gluon from the proton couple to a heavy quark-antiquark pair. Heavy meson production thus depends on the gluon content of the proton. As the heavy quark mass is non-negligible compared to the scale  $Q$ , set by the exchanged virtual photon, theoretical prediction need to include the quark masses. Measurements of the contributions from heavy quarks to the inclusive structure function,  $F_2^c$  and  $F_2^b$  hence provide both interesting tests of QCD and sensitivity to the gluon density. Figure 7 shows these contributions measured using a lifetime analysis: in addition to the scattered electron,

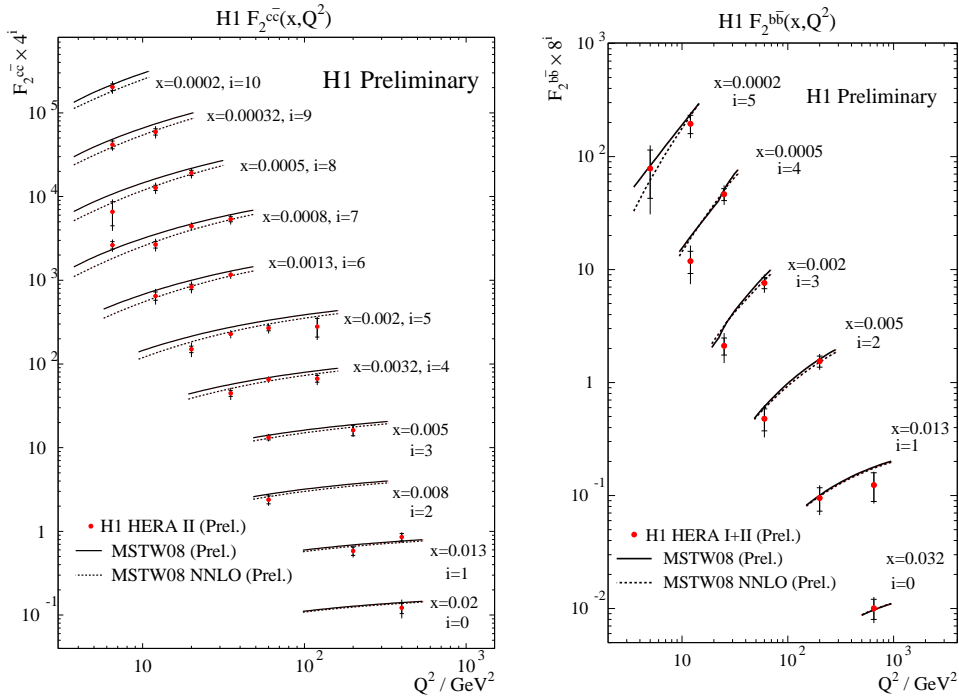


Figure 7: Contribution from charm and beauty production to the structure function  $F_2$ , measured with a lifetime analysis

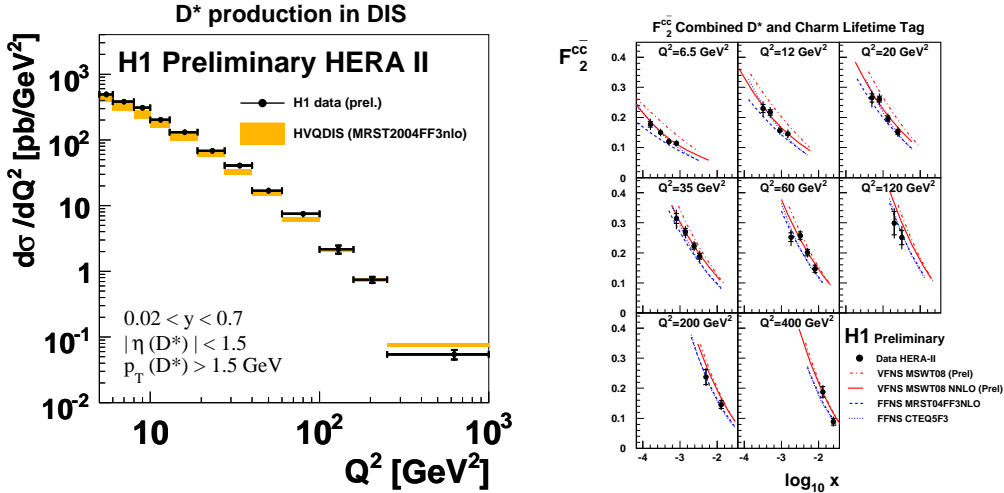


Figure 8: Cross-section for  $D^*$  meson production (left) and the structure function  $F_2^c$ , after averaging  $D^*$  and lifetime data (right)

tracks or vertexes significantly displaced from the primary vertex are required. The analysis covers the kinematic range  $5 < Q^2 < 650$  GeV. NLO QCD predictions are in agreement with these measurements.

Another way to experimentally access the charm contribution is by reconstructing  $D^*$  mesons. The production of  $D^*$  mesons is measured in the kinematic range  $5 < Q^2 < 800$  GeV. Good agreement with calculations is found, and the measurement is extrapolated to the full phase-space. Figure 8 shows the cross-section for  $D^*$  as a function of  $Q^2$  and the structure function  $F_2^c$  after combining the  $D^*$  data with the lifetime analysis. The structure function  $F_2^c$  is compared to QCD predictions based on different parameterisations of the parton densities. The QCD predictions are found to be in agreement with the combined  $F_2^c$  data. At low  $Q^2$  the data start to discriminate between various schemes of including heavy quark masses in the theory. The precision of the data is comparable with the spread in the theoretical predictions and prefigures further constraints on the proton structure.

## 5 Measurements of the hadronic final state

The production of jets at HERA provides a clean environment to study fundamental properties of QCD, like the strong coupling constant  $\alpha_s$ . The H1 collaboration measures inclusive jet production normalised to inclusive DIS, as well as the rate of 2-jet and 3-jet events [12]. The measurements are performed as a function of  $Q^2$  and  $\langle P_T \rangle$  in the kinematic range  $150 < Q^2 < 15000$  GeV<sup>2</sup>, where  $\langle P_T \rangle$  is the jet transverse momentum. A value  $\alpha_s = 0.1168 \pm 0.0007(\text{exp.})_{-0.0030}^{+0.0046}(\text{theor.}) \pm 0.0016(\text{PDF})$  is found in an NLO QCD analysis. The small experimental error on  $\alpha_s$  compared to the dominant theoretical error emphasises the need of higher order calculations for jet production at HERA. The running of  $\alpha_s$  with  $Q^2$ , as seen in jet production at HERA and a comparison to other  $\alpha_s$  measurements is shown

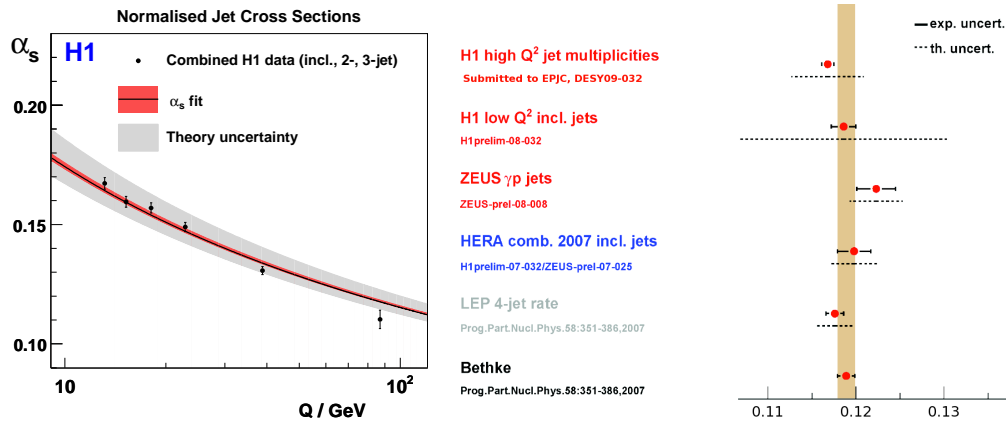


Figure 9: Measurements of  $\alpha_s$  from jets at HERA

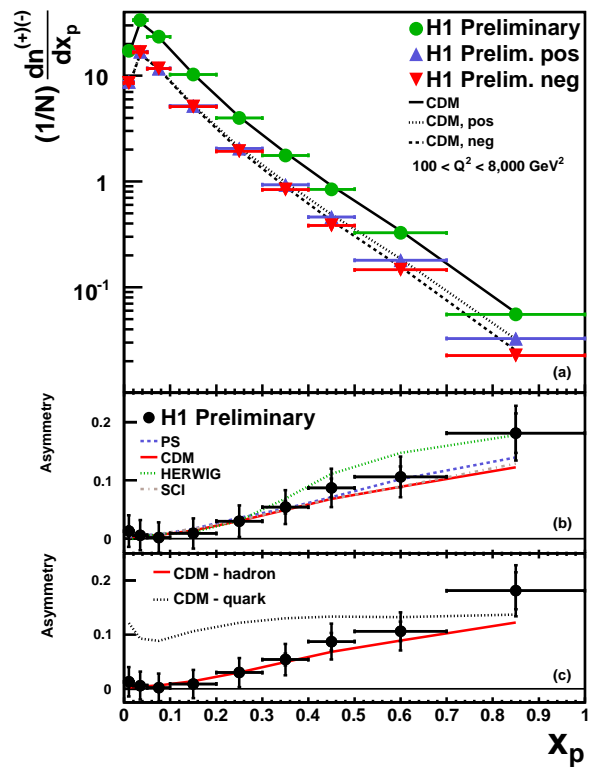


Figure 10: The particle charge asymmetry measured at HERA

in Figure 9.

As a further investigation of QCD effects in the hadronic final state structure, the production of charged particles is studied. The charged particle spectra are sensitive to the fragmentation process, in which hadrons are produced from the initial state partons. As opposed to the hard process, which can be calculated in perturbation theory, fragmentation is described by phenomenological models. H1 measured the production of charged particles [13] as a function of  $x_p$ , the momentum fraction in the current hemisphere of the Breit frame, in the kinematic range  $100 < Q^2 < 20000 \text{ GeV}$ . More insights in the fragmentation process are obtained by studying particle production separately for negatively and positively charged particles. These rates and the associated asymmetry are shown in Figure 10. The asymmetry is small at low  $x_p$  and rises up to 0.18 for high  $x_p$ , in agreement with various fragmentation models. In contrast, the charge asymmetry observed at parton level, does not depend strongly on  $x_p$ .

## 6 Diffraction

Diffraction processes contribute at a level of about 10% to the DIS cross-sections at HERA. They are characterised by the fact that the proton stays intact or fragments into a system with small mass  $M_Y$ , even though a second hadronic system is produced. This is interpreted

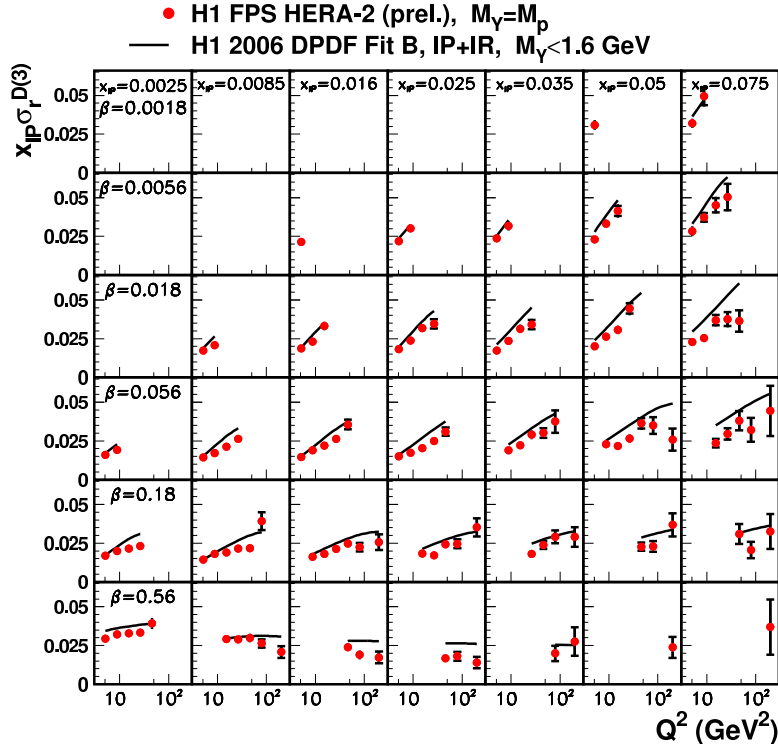


Figure 11: Leading proton data on  $x_{IP}\sigma_R$



as the exchange of a colour-neutral hadronic object. In leading order QCD, this is explained by the exchange of two gluons. Experimentally, diffractive events are detected by identifying the outgoing proton or by requiring a large rapidity gap free of hadronic activity and separating the two hadronic systems. New results on inclusive diffraction are derived from data taken with the H1 Forward Proton Spectrometer (FPS). Leading protons are detected in the FPS, which is located about 80 m downstream the main H1 detector in the HERA tunnel, using roman pot detectors inside the evacuated part of the beam transport system. Compared to earlier measurements with a leading proton [15], the analysed data sample corresponds to an integrated luminosity increased by one order of magnitude. The resulting reduced cross-section is shown in Figure 11 as a function of three variables:  $x_{\text{IP}}$ ,  $\beta$  and  $Q^2$ . The variable  $\beta$  is related to Bjorken  $x$  and the momentum fraction  $x_{\text{IP}}$  of the colourless object entering the hard interaction,  $\beta = x/x_{\text{IP}}$ . The data are compared to predictions from a QCD fit to inclusive H1 rapidity gap data [14]. Agreement is found, taking into account the fact that the fit includes data up to a mass  $M_Y < 1.6$  GeV, whereas the new data are collected with a leading proton, i.e.  $M_Y = M_p$ . Compared to [15], the new measurements extend to higher  $Q^2$ . The precision reached is of order 8% at low  $Q^2$ , limited by systematic effects.

A first measurement of the diffractive longitudinal structure function  $F_L^D$  is performed,

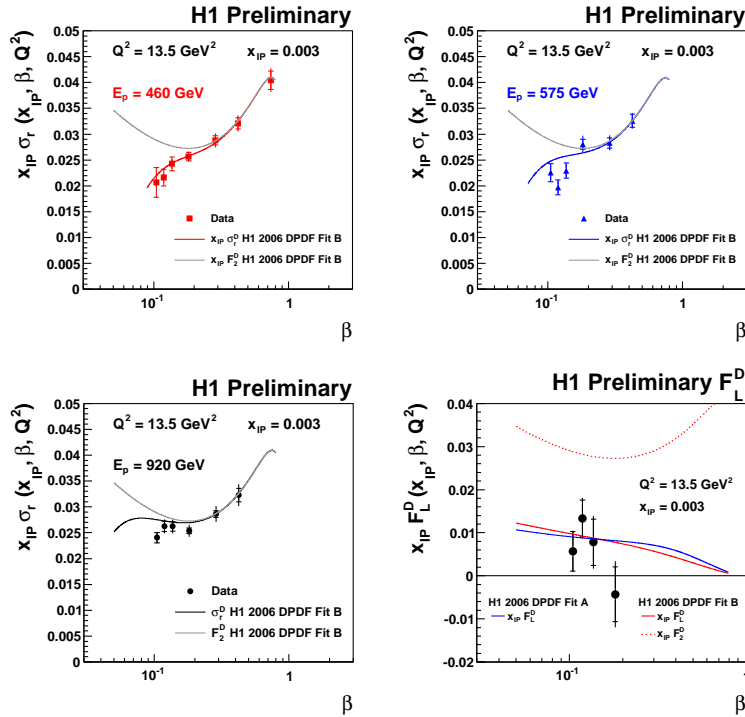


Figure 12: The diffractive reduced cross-section  $x_{\text{IP}} \sigma_r$ , measured for three centre-of-mass energies and the extracted structure function  $F_L^D$  (lower left)

using data collected in the low energy runs. The diffractive reduced cross section  $x_{\text{IP}}\sigma_r$  is decomposed into a linear combination of the structure functions  $F_2^D$  and  $F_L^D$ . The contribution from  $F_2^D$  is independent of the centre-of-mass energy, in contrast to the contribution proportional to  $F_L^D$ . Thus, by analysing  $x_{\text{IP}}\sigma_r$  at various beam energies,  $F_L^D$  is extracted. The quantity  $x_{\text{IP}}\sigma_r$  for various beam energies and the resulting structure function  $F_L^D$  are shown as a function of  $\beta$  in Figure 12. The  $F_L^D$  data agree with predictions derived from the diffractive PDF fit [14] to inclusive H1 data.

It is also interesting to look for the production of leading neutrons, which are produced from an electrically charged, colourless exchange with the proton. Such neutrons are detected in the Forward Neutron Calorimeter (FNC) located 106 m from the main detector in the HERA tunnel. Compared to earlier measurements [16], the new data profit from much increased integrated luminosity and an improved FNC. Figure 13 shows the measured structure function  $F_2^{LN}$  as a function of the three variables Bjorken  $x$ ,  $Q^2$  and  $x_L$ , where  $x_L$  is the neutron energy, normalised to the proton beam energy. The data are compared to predictions from two Monte Carlo (MC) models: DJANGO, where leading neutrons are produced in the fragmentation process, and RAPGAP  $\pi^+$  where leading neutrons are produced by the exchange of a charged pion. After applying global normalisation constants, the sum of these MC models is able to describe the data. Also shown in Figure 13 are the  $F_2^{LN}$  data at  $x_L = 0.73$  divided by a corresponding pion flux factor  $\Gamma_\pi = 0.131$ . At high  $x_L$  the data are dominated by the pion exchange, and hence the pion structure function may be extracted. The  $F_2^{LN}$  data divided by the pion flux factor compare well in shape to various parameterisations of the pion structure function.

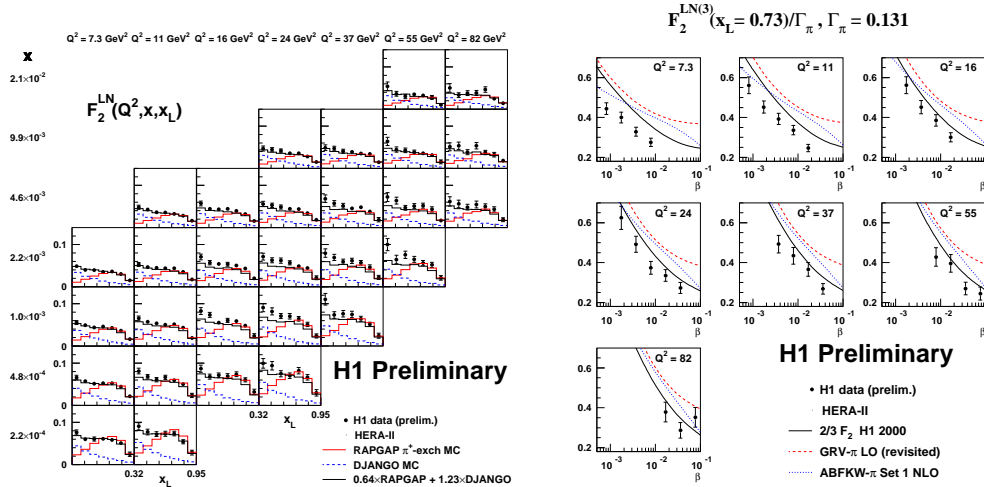


Figure 13: The structure function  $F_2^{LN}$  with a leading neutron (left) and comparisons to parameterisations of the pion structure function (right)

## 7 Summary

The H1 collaboration has presented a wealth of new results based on the datasets collected until mid 2007. A selection of these results in the areas searches for new physics, structure functions, heavy flavour production, hadronic final states and diffraction are discussed.

Most searches have now been completed, using the full HERA statistics. The combination of H1 and ZEUS data has started, in order to reach the best possible sensitivity to physics beyond the standard model.

The precision of inclusive cross-sections data measured by H1 is now as good as 1.3 – 2% in the bulk of the phase-space, opening new possibilities for QCD fits. The structure function  $F_L$  is measured over the full  $Q^2$  range available at HERA. Of particular interest is the region of lowest  $Q^2$ , where the models diverge most and the data start to discriminate amongst them.

Using the H1 vertex-detector, contributions from charm and beauty to the inclusive structure function  $F_2$  are extracted. In combination with data from  $D^*$  decays, the data show sensitivity to the heavy flavour treatment in QCD fits and may contribute to further constrain the proton structure.

New measurements of jet production at high  $Q^2$  lead to very small experimental errors on the strong coupling  $\alpha_s$ . Higher order calculations are needed to pin down the theory errors. The charged particle asymmetry of the scattered hadronic final state is observed for the first time in  $ep$  collisions and found in agreement with predictions based on phenomenological models.

A measurement of the diffractive longitudinal structure function  $F_L^D$  is presented here for the first time. Diffractive PDF fits to inclusive H1 data are in agreement with this new data. Using dedicated detectors FPS and FNC the production of leading protons and leading neutrons, respectively, is measured. The new leading proton data extend the kinematic range and have superior precision as compared to earlier measurements. They are in agreement with predictions of the diffractive PDF fit. The leading neutron data can be used to test fragmentation models and to extract the pion structure function.

The results presented here reveal the potential of the full HERA physics data, which will continue to be exploited in the next years.

## References

- [1] Slides:  
<http://indico.cern.ch/contributionDisplay.py?contribId=1&sessionId=6&confId=53294>
- [2] F. D. Aaron *et al.* [H1 Collaboration], submitted to EPJC, arXiv:0901.0488.
- [3] F. D. Aaron *et al.* [H1 Collaboration], Phys. Lett. B **668** (2008) 268 [arXiv:0806.3987 [hep-ex]].
- [4] Z. Collaboration, arXiv:0906.1504 [hep-ex].
- [5] T. H. Collaboration and t. Z. Collaboration, arXiv:0907.3627 [hep-ex].
- [6] F. D. Aaron *et al.* [H1 Collaboration], Phys. Lett. B **663** (2008) 382 [arXiv:0802.1858 [hep-ex]].
- [7] F. D. Aaron *et al.* [H1 Collaboration], Phys. Lett. B **666** (2008) 131 [arXiv:0805.4530 [hep-ex]].
- [8] H. Collaboration, arXiv:0904.3392 [hep-ex].
- [9] H. Collaboration, arXiv:0904.0929 [hep-ex].
- [10] H. Collaboration, arXiv:0904.3513 [hep-ex].
- [11] F. D. Aaron *et al.* [H1 Collaboration], Phys. Lett. B **665** (2008) 139 [arXiv:0805.2809 [hep-ex]].
- [12] H. Collaboration, arXiv:0904.3870 [hep-ex].

- [13] F. D. Aaron *et al.* [H1 Collaboration], Phys. Lett. B **654** (2007) 148 [arXiv:0706.2456 [hep-ex]].
- [14] A. Aktas *et al.* [H1 Collaboration], Eur. Phys. J. C **48** (2006) 715 [arXiv:hep-ex/0606004].
- [15] A. Aktas *et al.* [H1 Collaboration], Eur. Phys. J. C **48** (2006) 749 [arXiv:hep-ex/0606003].
- [16] C. Adloff *et al.* [H1 Collaboration], Eur. Phys. J. C **6** (1999) 587 [arXiv:hep-ex/9811013].